

# Atypical protein kinase C iota (PKC $\iota$ ) ensures mammalian development by establishing the maternal-fetal exchange interface.

著者	Bhaswati Bhattacharya, Pratik Home, Avishek Ganguly, Soma Ray, Ananya Ghosh, Md Rashedul Islam, Valerie French, Courtney Marsh, Sumedha Gunewardena, Hiroaki Okae, Takahiro Arima, Soumen Paul
journal or publication title	Proceedings of the National Academy of Sciences of the United States of America
volume	117
number	25
page range	14280-14291
year	2020-06-08
URL	<a href="http://hdl.handle.net/10097/00130842">http://hdl.handle.net/10097/00130842</a>

doi: 10.1073/pnas.1920201117



# Atypical protein kinase C iota (PKC $\lambda/i$ ) ensures mammalian development by establishing the maternal–fetal exchange interface

Bhaswati Bhattacharya<sup>a</sup>, Pratik Home<sup>a,b</sup>, Avishek Ganguly<sup>a</sup>, Soma Ray<sup>a</sup>, Ananya Ghosh<sup>a</sup>, Md. Rashedul Islam<sup>a</sup>, Valerie French<sup>b,c</sup>, Courtney Marsh<sup>b,c</sup>, Sumedha Gunewardena<sup>d</sup>, Hiroaki Okae<sup>e</sup>, Takahiro Arima<sup>e</sup>, and Soumen Paul<sup>a,b,c,1</sup>

<sup>a</sup>Department of Pathology and Laboratory Medicine, University of Kansas Medical Center, Kansas City, KS 66160; <sup>b</sup>Institute for Reproduction and Perinatal Research, University of Kansas Medical Center, Kansas City, KS 66160; <sup>c</sup>Department of Obstetrics and Gynecology, University of Kansas Medical Center, Kansas City, KS 66160; <sup>d</sup>Department of Molecular and Integrative Physiology, University of Kansas Medical Center, Kansas City, KS 66160; and <sup>e</sup>Department of Informative Genetics, Environment and Genome Research Center, Tohoku University Graduate School of Medicine, Sendai 980-8575, Japan

Edited by Thomas E. Spencer, University of Missouri, Columbia, MO, and approved May 5, 2020 (received for review November 18, 2019)

In utero mammalian development relies on the establishment of the maternal–fetal exchange interface, which ensures transportation of nutrients and gases between the mother and the fetus. This exchange interface is established via development of multinucleated syncytiotrophoblast cells (SynTs) during placentation. In mice, SynTs develop via differentiation of the trophoblast stem cell-like progenitor cells (TSPCs) of the placenta primordium, and in humans, SynTs are developed via differentiation of villous cytotrophoblast (CTB) progenitors. Despite the critical need in pregnancy progression, conserved signaling mechanisms that ensure SynT development are poorly understood. Herein, we show that atypical protein kinase C iota (PKC $\lambda/i$ ) plays an essential role in establishing the SynT differentiation program in trophoblast progenitors. Loss of PKC $\lambda/i$  in the mouse TSPCs abrogates SynT development, leading to embryonic death at approximately embryonic day 9.0 (E9.0). We also show that PKC $\lambda/i$ -mediated priming of trophoblast progenitors for SynT differentiation is a conserved event during human placentation. PKC $\lambda/i$  is selectively expressed in the first-trimester CTBs of a developing human placenta. Furthermore, loss of PKC $\lambda/i$  in CTB-derived human trophoblast stem cells (human TSCs) impairs their SynT differentiation potential both in vitro and after transplantation in immunocompromised mice. Our mechanistic analyses indicate that PKC $\lambda/i$  signaling maintains expression of GCM1, GATA2, and PPAR $\gamma$ , which are key transcription factors to instigate SynT differentiation programs in both mouse and human trophoblast progenitors. Our study uncovers a conserved molecular mechanism, in which PKC $\lambda/i$  signaling regulates establishment of the maternal–fetal exchange surface by promoting trophoblast progenitor-to-SynT transition during placentation.

placenta | human trophoblast stem cell | cytotrophoblast syncytiotrophoblast | protein kinase C $\lambda/i$

Trophoblast progenitors are critical for embryo implantation and early placentation. Defective development and differentiation of trophoblast progenitors during early human pregnancy either leads to pregnancy failure (1–4), or pregnancy-associated complications like fetal growth restriction and preeclampsia (3–6), or serves as the developmental cause for postnatal or adult diseases (7–9). However, due to experimental and ethical barriers, we have a poor understanding of molecular mechanisms that are associated with early stages of human placentation. Rather, gene knockout (KO) studies in mice have provided important information about molecular mechanisms that regulate mammalian placentation. While mouse and human placentae differ in their morphology and trophoblast cell types, important similarities exist in the formation of the maternal–fetal exchange interface. Both mice and humans display hemochorial placentation (10), where the maternal–fetal exchange interface is established via direct contact between maternal blood and placental syncytiotrophoblast cells (SynTs).

In a periimplantation mouse embryo, proliferation and differentiation of polar trophoblast results in the formation of trophoblast stem cell-like progenitor cells (TSPCs), which reside within the extraembryonic ectoderm ExE (11), and later in ExE-derived ectoplacental cone (EPC) and chorion. Subsequently, the TSPCs within the ExE/EPC region contribute to develop the junctional zone, a compact layer of cells sandwiched between the labyrinth and the outer trophoblast giant cell (TGC) layer. Development of the junctional zone is associated with differentiation of trophoblast progenitors to four trophoblast cell lineages: 1) TGCs (12), 2) spongiotrophoblast cells (13), 3) glycogen cells, and 4) invasive trophoblast cells that invade the uterine wall and maternal vessels (14–16).

The mouse placental labyrinth, which constitutes the maternal–fetal exchange interface, develops after the allantois attaches with the chorion. The multilayered chorion forms around embryonic day 8.0 (E8.0) when chorionic ectoderm fuses to basal EPC, thereby reuniting TSPC populations separated by formation of the ectoplacental cavity (17). Subsequently, the chorion attaches with the allantois to initiate the development of the placental labyrinth, which contains two layers of SynTs, known as SynT-I and SynT-II. At

## Significance

Successful embryonic development relies on proper nutrient and gas exchange between the mother and the fetus. Here, we showed that the atypical protein kinase C isoform, PKC $\lambda/i$ , mediates an evolutionarily conserved function to establish the maternal–fetal exchange interface during in utero mammalian development. Using human trophoblast stem cells and genetic mouse models, our molecular analyses identified a PKC $\lambda/i$ -dependent, evolutionarily conserved gene expression program that instigates differentiation in trophoblast progenitors of a developing mammalian placenta to establish the maternal–fetal exchange interface.

Author contributions: B.B. and S.P. designed research; B.B., P.H., A. Ganguly, S.R., A. Ghosh, and M.R.I. performed research; V.F., C.M., H.O., and T.A. contributed new reagents/analytic tools; S.G. analyzed genomics data; and B.B. and S.P. wrote the paper.

The authors declare no competing interest.

This article is a PNAS Direct Submission.

This open access article is distributed under [Creative Commons Attribution-NonCommercial-NoDerivatives License 4.0 \(CC BY-NC-ND\)](https://creativecommons.org/licenses/by-nc-nd/4.0/).

Data deposition: The raw data for RNA-sequencing analyses with mouse trophoblast stem cells, with or without the knockdown of *Prkci* gene, which encodes the atypical protein kinase C $\lambda/i$  isoform, have been deposited in the Gene Expression Omnibus (GEO) database (accession no. [GSE100285](https://www.ncbi.nlm.nih.gov/geo/query/acc.cgi?acc=GSE100285)).

<sup>1</sup>To whom correspondence may be addressed. Email: [spaul2@kumc.edu](mailto:spaul2@kumc.edu).

This article contains supporting information online at <https://www.pnas.org/lookup/suppl/doi:10.1073/pnas.1920201117/-DCSupplemental>.

First published June 8, 2020.

the onset of labyrinth formation, glial cells missing 1 (*Gcm1*) expression is induced in the TSPCs of the chorionic ectoderm (18), which promotes cell cycle exit and differentiation to the SynT-II lineage (17), whereas the TSPCs of the basal EPC progenitors that express Distal-less 3 (*Dlx3*) contribute to syncytial SynT-I lineage (17).

In contrast to mice, the earliest stage of human placentation is associated with the formation of a zone of invasive primitive syncytium at the blastocyst implantation site (19–21). Later, columns of cytotrophoblast cell (CTB) progenitors penetrate the primitive syncytium to form primary villi. With the progression of pregnancy, primary villi eventually branch and mature to form the villous placenta, containing two types of matured villi: 1) anchoring villi, which anchor to maternal tissue, and 2) floating villi, which float in the maternal blood of the intervillous space (19–21). The proliferating CTBs within anchoring and floating villi adapt distinct differentiation fates during placentation (22). In anchoring villi, CTBs establish a column of proliferating CTB progenitors known as column CTBs (22), which differentiate to invasive extravillous trophoblasts (EVTs), whereas CTB progenitors of floating villi (villous CTBs) differentiate and fuse to form the outer multinucleated SynT layer. The villous CTB-derived SynTs establish the nutrient, gas, and waste exchange surface, produce hormones, and promote immune tolerance to fetus throughout gestation (23–28).

Thus, the establishment of the placental exchange surface in both mice and humans are associated with the formation of differentiated, multinucleated SynTs from the trophoblast progenitors of placenta primordia. Moreover, both mouse and human trophoblast progenitors express key transcription factors, such as GCM1, DLX3, peroxisome proliferator-activated nuclear receptor gamma (PPAR $\gamma$ ), and GATA binding protein 2 (GATA2), which have been shown to be important for SynT development during placentation (1–4, 29–33). Despite these similarities, conserved signaling pathways that program SynT development in both mouse and human trophoblast progenitors are incompletely understood. Fortunately, the success in deriving true human trophoblast stem cells (TSCs) from villous CTBs (34) have opened up possibilities for direct assessment of conserved mechanisms that prime differentiation of multipotent trophoblast progenitor to SynT lineage. Therefore, we herein analyzed both mouse mutants and human TSCs to test the specific role of PKC $\lambda/1$  in that process.

The PKC $\lambda/1$  belongs to the atypical group of PKCs, which consists of another isoform PKC $\zeta$ . The aPKC isoforms have been implicated in cell lineage patterning in preimplantation embryos (35). We demonstrated that both PKC $\zeta$  and PKC $\lambda/1$  regulate self-renewal vs. differentiation potential in both mouse and rat embryonic stem cells (36–38). Interestingly, gene KO studies in mice indicated that PKC $\zeta$  is dispensable for embryonic development (39), whereas ablation of PKC $\lambda/1$  results in early gestation abnormalities leading to embryonic lethality (40, 41) prior to E9.5, a developmental stage equivalent to first trimester in humans. However, the importance of PKC $\lambda/1$  in the context of postimplantation trophoblast lineage development during mouse or human placentation has never been addressed. We found that PKC $\lambda/1$  protein is specifically abundant in TSPCs and villous CTBs within the developing mouse and human placenta, respectively. We show that both global and trophoblast-specific loss of PKC $\lambda/1$  in a mouse embryo is associated with defective development of placental labyrinth due to impairment of gene expression programming that ensures SynT development. We further demonstrate that the PKC $\lambda/1$  signaling in human TSCs is also essential for maintaining their SynT differentiation potential. Our analyses revealed an evolutionarily conserved, developmental-stage-specific mechanism in which PKC $\lambda/1$ -signaling orchestrates gene expression program in trophoblast progenitors for successful progression of in utero mammalian development.

## Results

**PKC $\lambda/1$  Protein Expression Is Selectively Abundant in the Trophoblast Progenitors of Developing Mouse and Human Placentae.** Earlier studies showed that PKC $\lambda/1$  is ubiquitously expressed in all cells of a developing preimplantation mouse embryo (42), including the trophoblast cells. Also, another study showed that PKC $\lambda/1$  is ubiquitously expressed in both embryonic and extraembryonic cell lineages in a postimplantation E7.5 mouse embryo (41). We validated both of these observations in a blastocyst (*SI Appendix, Fig. S1A*) and in E7.5 mouse embryo (*SI Appendix, Fig. S1B*). However, relative abundance of PKC $\lambda/1$  protein expression in different cell types is not well documented during postimplantation mouse development. Therefore, we tested PKC $\lambda/1$  protein expression at different stages of mouse postimplantation development. We found that in approximately E8 mouse embryos, PKC $\lambda/1$  protein is most abundantly expressed in the TSPCs residing in the placenta primordium (Fig. 1A). In comparison, cells within the developing embryo proper showed very low levels of PKC $\lambda/1$  protein expression. The high abundance of *Prkci* mRNA and PKC $\lambda/1$  protein expression was detected in the trophoblast cells of an E9.5 mouse embryo (*SI Appendix, Fig. S1C* and Fig. 1B). We also observed that PKC $\lambda/1$  is expressed in the maternal decidua. Surprisingly, the embryo proper showed extremely low PKC $\lambda/1$  protein expression at this developmental stage. The abundance of PKC $\lambda/1$  protein expression in the trophoblast is also maintained as development progresses. However, cells in the embryo proper also show PKC $\lambda/1$  protein expression beginning at midgestation as in E12.5 (*SI Appendix, Fig. S1D*).

As PKC $\lambda/1$  expression during human placentation has never been tested, we investigated PKC $\lambda/1$  protein expression in human placenta at different stages of gestation. Our analyses revealed that PKC $\lambda/1$  protein is expressed specifically in the villous CTBs within a first-trimester human placenta (Fig. 1C). PKC $\lambda/1$  is also expressed in CTBs within term placenta (Fig. 1C). To further quantitate PKC $\lambda/1$  expression, we isolated CTBs from first-trimester and term placenta and analyzed *PRKCI* mRNA expression. We also isolated SynT from term placenta via laser capture microdissection (*SI Appendix, Fig. S1E*). We found that *PRKCI* mRNA expression is approximately twofold higher in first-trimester CTBs compared to that in term CTBs (*SI Appendix, Fig. S1F*). However, PKC $\lambda/1$  expression is strongly repressed in differentiated SynTs in first-trimester human placenta (Fig. 1C) as well as in term placenta (*SI Appendix, Fig. S1F*).

**Global Loss of PKC $\lambda/1$  in a Developing Mouse Embryo Abrogates Placentation.** Global deletion of *Prkci* in a developing mouse embryo (PKC $\lambda/1$  KO embryo) results in gastrulation defect leading to embryonic lethality (40, 41) at approximately E9.5. However, the placentation process was never studied in PKC $\lambda/1$  KO mouse embryos. As many embryonic lethal mouse mutants are associated with placentation defects, we probed into trophoblast development and placentation in postimplantation PKC $\lambda/1$  KO embryos. We started investigating placenta and trophoblast development in PKC $\lambda/1$  KO embryos starting from E7.5. At this stage, the placenta primordium consists of the ExE/EPC regions. However, we did not notice any obvious phenotypic differences of the ExE/EPC development between the control and the PKC $\lambda/1$  KO embryos at E7.5 (Fig. 2A, *Left*, and *SI Appendix, Fig. S2A*). We noticed developmental defect in PKC $\lambda/1$  KO placenta after the chorio-allantoic attachment, an event which takes place at approximately E8.5. We noticed that PKC $\lambda/1$  KO developing placenta were smaller in size at E8.5 (Fig. 2A, *Middle*), and this defect in placentation was more prominent in E9.5 embryos. At E9.5, the placenta in PKC $\lambda/1$  KO embryos were significantly smaller in size (Fig. 2A, *Right*, and *SI Appendix, Figs. S2A and S3A*), and the embryo proper also showed gross impairment in development and was significantly

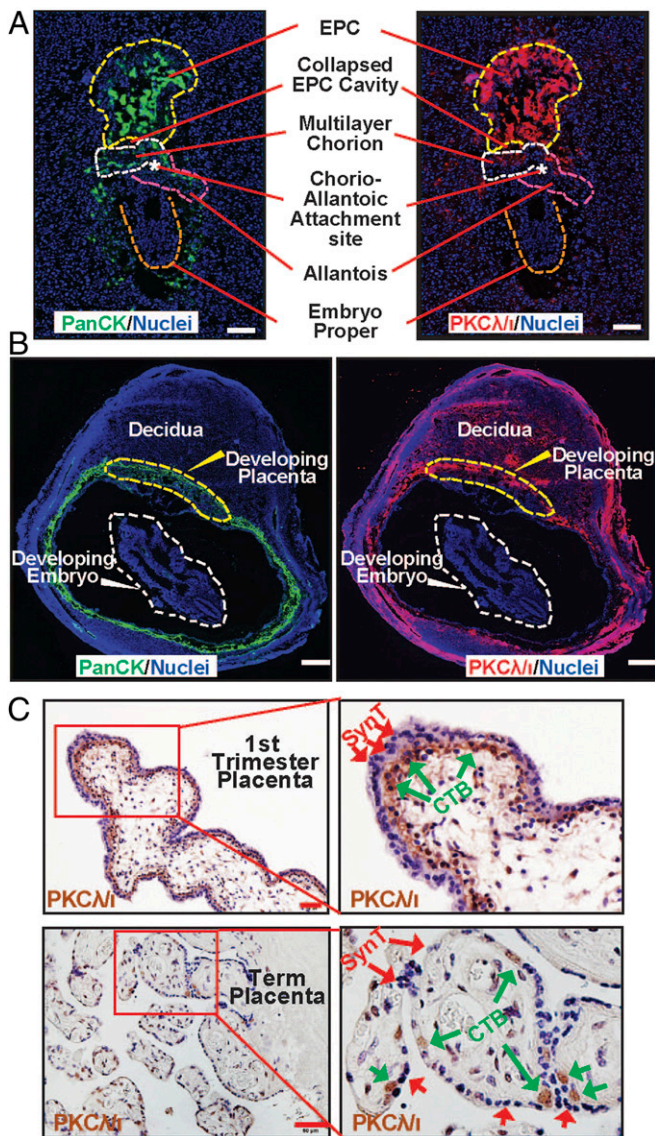


**Fig. 1.** PKC $\lambda/\iota$  protein expression is selectively abundant in trophoblast progenitors of early postimplantation mammalian embryos. (A) Immunofluorescence images showing trophoblast progenitors, marked by anti-cytokeratin antibody (green), expressing high levels of PKC $\lambda/\iota$  protein (red) in an approximately E8 mouse embryo. Note much less expression of PKC $\lambda/\iota$  protein within cells of the developing embryo proper (orange dotted boundary). EPC, chorion, allantois, and the chorio-allantoic attachment site are indicated with yellow, white, and pink dotted lines, and a white asterisk, respectively. (Scale bars, 100  $\mu$ m.) (B) Immunofluorescence images of an E9.5 mouse implantation sites showing pan-cytokeratin (Left), PKC $\lambda/\iota$  (Right), and nuclei (DAPI). At this developmental stage, PKC $\lambda/\iota$  protein is highly expressed in trophoblast cells of the developing placenta and in maternal uterine cells. However, PKC $\lambda/\iota$  protein expression is much less in the developing embryo. (Scale bars, 500  $\mu$ m.) (C) Immunohistochemistry showing PKC $\lambda/\iota$  is selectively expressed within the cytotrophoblast progenitors (green arrows) of first-trimester (8 wk) and term (38 wk) human placentae. (Scale bars, 50  $\mu$ m.)

smaller in size (Fig. 2B and SI Appendix, Figs. S24 and S34), as reported in earlier studies (40). Immunofluorescence analyses revealed defective embryonic–extraembryonic attachment with an altered orientation of the embryo proper with respect to the developing placenta (Fig. 2C).

We also failed to detect any visible labyrinth zone in most of the PKC $\lambda/\iota$  KO placentae. The abrogation of the placental

labyrinth and the SynT development were confirmed by a near-complete absence of *Gcm1* mRNA expression (SI Appendix, Fig. S2B) and lack of any *Dlx3*-expressing labyrinth trophoblast cells in E9.5 PKC $\lambda/\iota$  KO placentae (Fig. 2D). In contrast, the PKC $\lambda/\iota$  KO placentae mainly contained proliferin (PLF)-expressing TGCs (SI Appendix, Fig. S3A).

In a very few PKC $\lambda/\iota$  KO placentae (3 out of 32 analyzed by sectioning), other trophoblast cells exist along with TGCs (SI Appendix, Fig. S3A, red border). We tested the presence of different trophoblast subtypes in those placentae. We detected trophoblast-specific protein alpha (*Tpbpa*)-expressing spongiotrophoblast population (SI Appendix, Fig. S3B). We also tested for SynT markers. In a mouse placenta the matured labyrinth contains two layers of SynTs, SynT-I and SynT-II. The SynT-I cells express the retroviral gene syncytin A (*SynA*) (43), whereas the SynT-II population arises from *GCM1*-expressing progenitors (17). So, we tested presence of those cells via in situ hybridization. We detected the presence of some *SynA*-expressing cells (SI Appendix, Fig. S3B). However, we could not detect any *Gcm1*-expressing cells in any of the PKC $\lambda/\iota$  KO placenta (SI Appendix, Fig. S3B). We further tested formation of SynT-I and SynT-II layers by analyzing expressions of solute carrier family 16 member 1 (MCT1) and solute carrier family 16 member 3 (MCT4), respectively (44). In contrast to control placentae, in which we detected development of two MCT1 and MCT4-expressing SynT layers (SI Appendix, Fig. S3C), we only detected a few MCT1-expressing cells in PKC $\lambda/\iota$  KO placentae. However, those cells were dispersed, indicating lack of cell fusion and formation of a matured SynT-I layer. We could not detect any MCT4-expressing SynT-II cells in PKC $\lambda/\iota$  KO placentae. These results indicated that loss of PKC $\lambda/\iota$  leads to abrogation of SynT-II development. Although a few *SynA*/*MCT1*-expressing SynT-I–like populations could arise in a few PKC $\lambda/\iota$  KO placentae, they do not differentiate to a matured SynT-I layer.

We could not test placentation in the PKC $\lambda/\iota$  KO embryos beyond E9.5 as these embryos and placentae begin to resorb at late gestational stages. Thus, from our findings, we concluded that the global loss of PKC $\lambda/\iota$  in a developing mouse embryo leads to defective placentation after the chorio-allantoic attachment due to impaired development of the SynT lineage, resulting in abrogation of placental labyrinth formation.

#### Trophoblast-Specific PKC $\lambda/\iota$ Depletion Impairs Mouse Placentation Leading to Embryonic Death.

Since we observed placentation defect in the global PKC $\lambda/\iota$  KO embryos, we next interrogated the importance of trophoblast cell-specific PKC $\lambda/\iota$  function in mouse placentation and embryonic development. Although a *Prkci*-conditional KO mouse model exists, we could not get access to that mouse. Therefore, we performed RNA interference (RNAi) using lentiviral-mediated gene delivery approach as described earlier (45) to specifically deplete PKC $\lambda/\iota$  in the developing trophoblast cell lineage. We transduced zona-removed mouse blastocysts with lentiviral particles with short hairpin RNA (shRNA) against *Prkci* (Fig. 3A) and transferred them to pseudopregnant females. We confirmed the efficiency of shRNA-mediated PKC $\lambda/\iota$  depletion by measuring *Prkci* mRNA expression in transduced blastocysts (Fig. 3B) and also by testing loss of PKC $\lambda/\iota$  protein expressions in trophoblast cells of developing placentae in multiple experiments (SI Appendix, Fig. S4 A and B). Intriguingly, the trophoblast-specific PKC $\lambda/\iota$  depletion also resulted in embryonic death before E9.5 due to severe defect in both placental and embryonic development (Fig. 3 C and D). Furthermore, the immunofluorescence analyses of trophoblast cells at approximately E9.5 confirmed defective placentation in the *Prkci* knockdown (KD) placentae, characterized with a near-complete absence of the labyrinth zone (Fig. 3E) and *Dlx3*-expressing SynT populations (Fig. 3F). However, similar to PKC $\lambda/\iota$  KO placentae, *Prkci* KD placentae predominantly

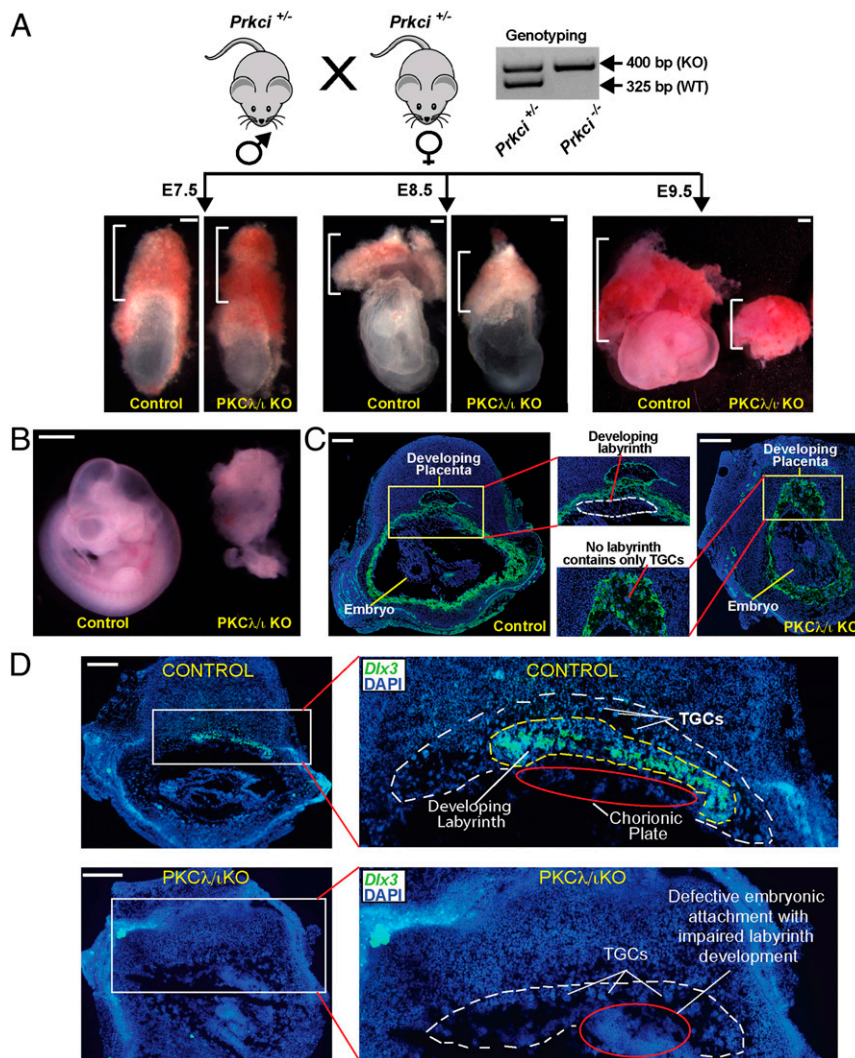


**Fig. 2.** Global Loss of PKC $\lambda/\iota$  in a developing mouse embryo abrogates placentation. (A) Experimental strategy and phenotype of mouse conceptuses defining the importance of PKC $\lambda/\iota$  in placentation. Heterozygous (*Prkci*<sup>+/-</sup>) male and female mice were crossed to generate homozygous KO (*Prkci*<sup>-/-</sup>, PKC $\lambda/\iota$  KO) embryos and confirmed by genotyping. Embryonic and placental developments were analyzed at E7.5, E8.5, and E9.5, and representative images are shown. At E7.5, placenta primordium developed normally in PKC $\lambda/\iota$  KO embryos. However, defect in placentation in PKC $\lambda/\iota$  KO conceptuses was observable (smaller placentae) at E8.5 and was prominent at E9.5. (Scale bars, 100  $\mu$ m.) (B) Developing control and PKC $\lambda/\iota$  KO embryos were isolated at approximately E9.5, and representative images are shown. The PKC $\lambda/\iota$  KO embryo proper shows gastrulation defect as described in an earlier study (40). (Scale bars, 500  $\mu$ m.) (C) Placentation at control and PKC $\lambda/\iota$  KO implantation sites were analyzed at approximately E9.5 via immunostaining with anti-pan-cytokeratin antibody (green, trophoblast marker). The developing PKC $\lambda/\iota$  KO placenta lacks the labyrinth zone and mainly contains the TGCs (red line). Also, unlike in control embryos, the developmentally arrested PKC $\lambda/\iota$  KO placenta and embryo proper are not segregated and are attached together. (Scale bars, 500  $\mu$ m.) (D) RNA in situ hybridization assay was performed using fluorescent probes against *Dlx3* mRNA. Images show that, unlike the control placenta, the PKC $\lambda/\iota$  KO placenta lacks *Dlx3*-expressing labyrinth trophoblast cells. (Scale bars, 500  $\mu$ m.)

contained PLF-expressing TGC populations (SI Appendix, Fig. S4C). Thus, the trophoblast-specific depletion of PKC $\lambda/\iota$  in a developing mouse embryo recapitulated similar placentation defect and embryonic death as observed in the global PKC $\lambda/\iota$  KO embryos.

**PKC $\lambda/\iota$  Signaling in a Developing Mouse Embryo Is Essential to Establish a Transcriptional Program for TSPC-to-SynT Differentiation.** The abrogation of labyrinth development in the trophoblast-specific *Prkci* KD mouse placentae indicated a critical importance of the PKC $\lambda/\iota$  signaling in SynT development and labyrinth formation. During mouse placentation, the SynT differentiation is associated with the suppression of TSC/TSPC-specific genes, such as caudal-type homeobox 2 (*Cbx2*), Eomesodermin (*Eomes*), TEA domain transcription factor 4 (*Tead4*), estrogen-related receptor beta (*Esr $\beta$* ), and E74-like

transcription factor 5 (*Elf5*) (2, 46–50), and induction of expression of the SynT-specific genes, such as *Gcm1*, *Dlx3*, and fusogenic retroviral genes SyncytinA and SyncytinB (3). In addition, other transcription factors, such as PPAR $\gamma$ , GATA transcription factors GATA2 and GATA3, and cell signaling regulators, including members of mitogen-activated protein kinase pathway, are implicated in mouse SynT development (32, 33, 51). Therefore, to define the molecular mechanisms of PKC $\lambda/\iota$ -mediated regulation of SynT development, we specifically depleted PKC $\lambda/\iota$  expression in mouse TSCs via RNAi (Fig. 4A) and asked whether the loss of PKC $\lambda/\iota$  impairs mouse TSC self-renewal or their differentiation to specialized trophoblast cell types.

When cultured in stem state culture condition (with FGF4 and heparin), PKC $\lambda/\iota$ -depleted mouse TSCs (*Prkci* KD mouse TSCs) did not show any defect in the stem state colony morphology (Fig. 4B). Also, cell proliferation analyses by MTT assay and

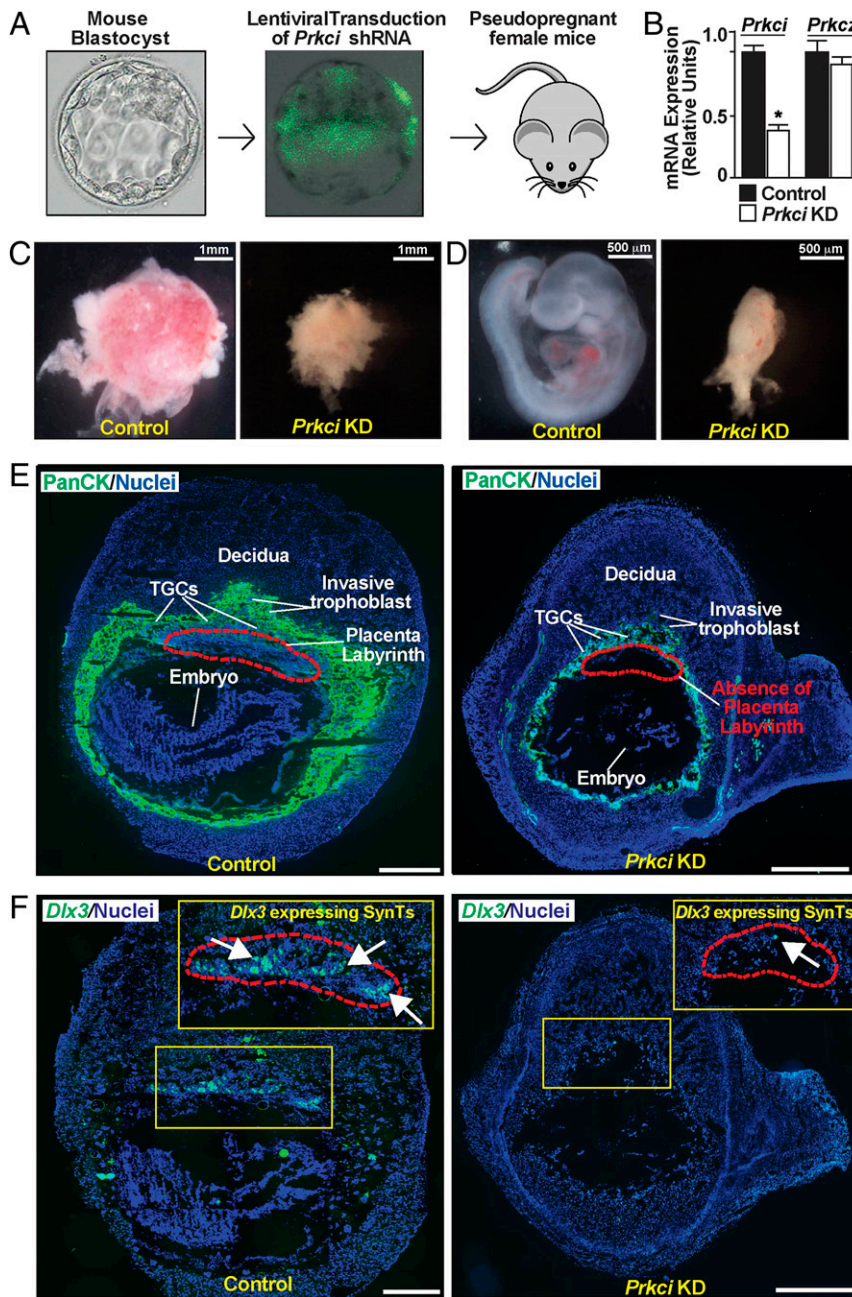


**Fig. 3.** Trophoblast-specific PKC $\lambda$ 1 depletion impairs mouse placentation leading to embryonic death. (A) Schematics to study developing mouse embryos with trophoblast-specific depletion of *Prkci* (*Prkci* KD embryos). Blastocysts were transduced with lentiviral vectors expressing shRNA against *Prkci*, and transduction was confirmed by monitoring EGFP expression. Transduced blastocysts were transferred into the uterine horns of pseudopregnant females to study subsequent effect on embryonic and placental development. (B) KD efficiency with shRNA was confirmed by testing loss of *Prkci* mRNA expression in transduced blastocysts. (C and D) Representative images show control and *Prkci* KD placentae and developing embryos, isolated at E9.5. Similar to global PKC $\lambda$ 1 KO embryos, trophoblast-specific *Prkci* KD embryos showed severe developmental defect. (E) Immunostaining with anti-pan-cytokeratin antibody (green, trophoblast marker) showed defective placentation in the *Prkci* KD implantation sites at approximately E9.5. The images show that, unlike the control placenta, labyrinth formation was abrogated in the *Prkci* KD placenta. (Scale bars, 500  $\mu$ m.) (F) RNA in situ hybridization assay confirmed near-complete absence of *Dlx3*-expressing trophoblast cells in the *Prkci* KD placenta. (Scale bars, 500  $\mu$ m.)

bromodeoxyuridine (BrdU) incorporation assay indicated that cell proliferation was not affected in the *Prkci* KD mouse TSCs (Fig. 4 C and D). Furthermore, mRNA expression analyses showed that expression of TSC stem state regulators, such as *Cdx2*, *Eomes*, *Gata3*, *Tead4*, *Esrrb*, and *Elf5* were not affected upon PKC $\lambda$ 1 depletion (Fig. 4E). Western blot analysis also confirmed that CDX2 protein expression was not affected in the *Prkci* KD TSCs (Fig. 4F). These results indicated that PKC $\lambda$ 1

signaling is not essential to maintain the self-renewal program in mouse TSCs.

Next, we asked whether the loss of PKC $\lambda$ 1 affects mouse TSC differentiation program. Removal of FGF4 and heparin from the culture medium induces spontaneous differentiation in mouse TSCs, which can be monitored over a course of 6 to 8 d. During this differentiation program, induction of SynT-differentiation markers like *Gcm1*, *Dlx3* can be monitored in

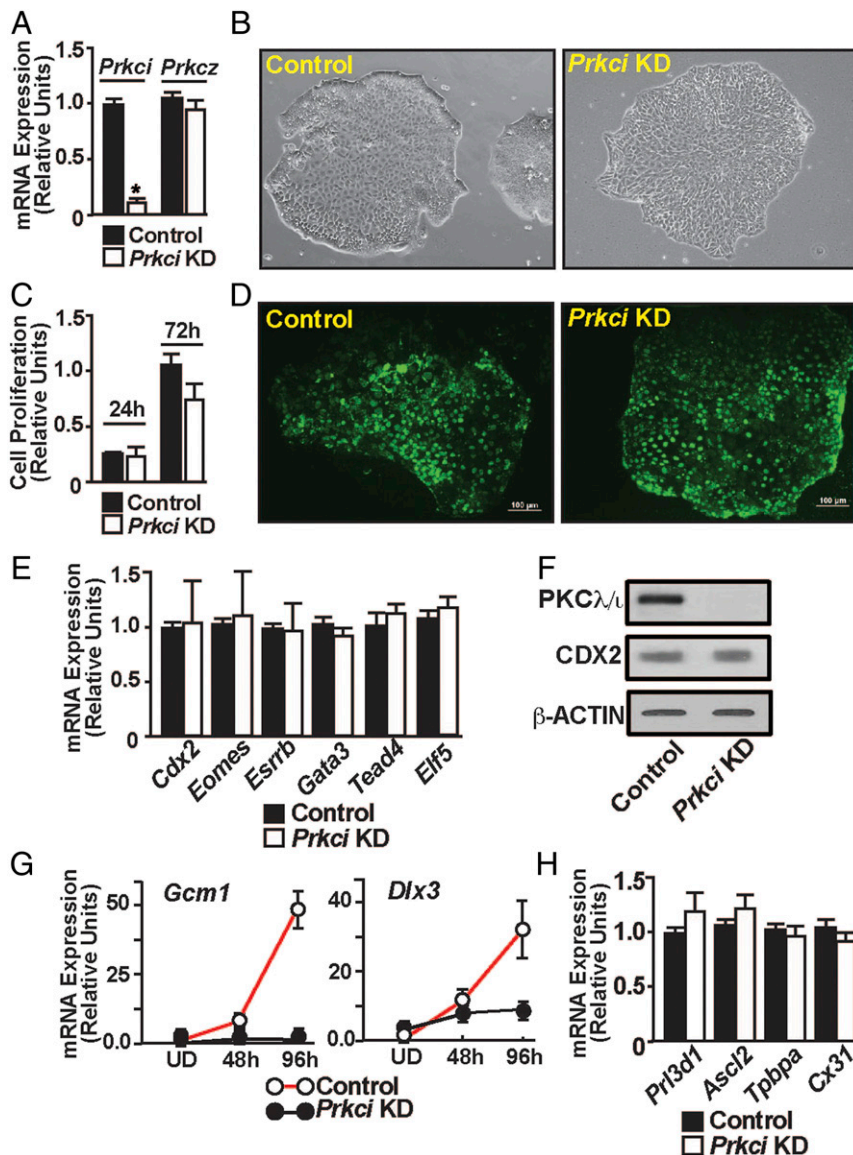


**Fig. 4.** PKC $\lambda$ 1 signaling is essential to establish a transcriptional program for SynT differentiation. (A) Quantitative RT-PCR to validate loss of *Prkci* mRNA expression in *Prkci* KD mouse TSCs (mean  $\pm$  SE;  $n = 4$ ,  $P \leq 0.001$ ). The shRNA molecules targeting the *Prkci* mRNA had no effect on *Prkcz* mRNA expression. (B) Morphology of control and *Prkci* KD mouse TSCs. (C and D) Assessing proliferation rate of control and *Prkci* KD mouse TSCs by MTT assay and BrdU labeling, respectively. (E) Quantitative RT-PCR (mean  $\pm$  SE;  $n = 3$ ), showing unaltered mRNA expression of trophoblast stem state-specific genes like *Cdx2*, *Eomes*, *Tead4*, *Gata3*, *Elf5*, and *Esrrb* in *Prkci* KD mouse TSCs. (F) Western blot analyses confirming unaltered CDX2 protein expression in mouse TSCs upon PKC $\lambda$ 1 depletion. (G) *Prkci* KD mouse TSCs were allowed to grow under differentiation conditions, and gene expression analyses of SynT markers *Gcm1* and *Dlx3* were done (mean  $\pm$  SE;  $n = 3$ ). The plots show that loss of PKC $\lambda$ 1 in mouse TSCs results in impaired induction of *Gcm1* and *Dlx3* expression. (H) Quantitative RT-PCR analyses of *Prl3d1*, *Ascl2*, *Tpbpa*, and *Cx31* mRNA expression in differentiated *Prkci* KD mouse TSCs (mean  $\pm$  SE;  $n = 3$ ) to assess TGCs, spongiotrophoblasts, and glycogen trophoblast cell differentiation, respectively. Expression of these genes was not altered in differentiated *Prkci* KD mouse TSCs, indicating PKC $\lambda$ 1 is dispensable for mouse TSC differentiation to TGCs, spongiotrophoblasts, and glycogen trophoblast cells.

differentiating cells between day 2 and day 4. Subsequently, the TSC markers are repressed in the differentiating TSCs as the TGC-specific differentiation program becomes more prominent. Thus, after day 6 of differentiation, mouse TSCs highly express TGC specific markers, like prolactin family 3 subfamily d member 1 (*Prl3d1*), heart and neural crest-derived transcript 1 (*Hand1*), and prolactin family 2 subfamily c member 2 (*Prl2c2*). In addition, trophoblast-specific protein alpha (*Tpbpa*), Achaete-scute homolog 2 (*Ascl2*), Connexin 31 (*Cx31*), which are markers of spongiotrophoblast and glycogen trophoblast cells of the placental junctional zone, are also induced in differentiated mouse TSCs.

As the loss of PKC $\lambda$ 1 affects labyrinth development, we monitored expressions of *Gcm1* and *Dlx3* in differentiating *Prkci* KD mouse TSCs. Similar to our findings with the PKC $\lambda$ 1-depleted placenta, induction of *Dlx3* and *Gcm1* mRNA expression was impaired in differentiating *Prkci* KD mouse TSCs (Fig. 4G). In contrast, induction of *Tpbpa*, *Prl3d1*, and *Cx31*, which are markers for spongiotrophoblasts, TGCs, and glycogen cells, respectively, were not affected in differentiated *Prkci* KD mouse TSCs (Fig. 4H). Thus, we concluded that the loss of PKC $\lambda$ 1 in mouse TSCs does not affect their differentiation to specialized trophoblast cells of the placental junctional zone, such as spongiotrophoblasts, TGCs, and the glycogen cells. Rather, PKC $\lambda$ 1 is

essential to specifically establish the SynT differentiation program in mouse TSCs.

Based on our findings with *Prkci* KD mouse TSCs, we hypothesized that the PKC $\lambda/1$  signaling might regulate key genes, which are specifically required to induce the SynT differentiation program in TSCs. To test this hypothesis, we performed unbiased whole RNA-sequencing (RNA-seq) analysis with *Prkci* KD mouse TSCs. RNA-seq analyses showed that the depletion of PKC $\lambda/1$  in mouse TSCs altered expression of 164 genes by at least twofold with a high significance level ( $P \leq 0.01$ ). Among these 164 genes, 120 genes were down-regulated and 44 genes were up-regulated (Fig. 5A and [Datasets S1](#) and [S2](#)). Ingenuity pathway analyses revealed multimodal biofunctions of PKC $\lambda/1$ -regulated genes, including involvement in embryonic and reproductive developments (Fig. 5B). To further gain confidence on PKC $\lambda/1$ -regulated genes in the mouse TSCs, we curated the number of altered genes with a false-discovery rate (FDR) threshold of 0.1. The FDR filtering identified only 6 up-regulated genes and 46 down-regulated genes in the *Prkci* KD mouse TSCs (Fig. 5C and [D](#) and [Dataset S3](#)). Among the down-regulated genes, *Prkci* was identified as the most significantly altered gene, thereby confirming the specificity and high efficiency of the shRNA-mediated *Prkci* depletion.

Among the six genes, which were significantly up-regulated in *Prkci* KD mouse TSCs, only growth differentiation factor 6 (*Gdf6*) has been implicated in trophoblast biology in an over-expression experiment with embryonic stem cells (52). However, *Gdf6* deletion in a mouse embryo does not affect placentation (53, 54). In contrast, three transcription factors, *Gata2*, *Pparg*, and *Cited2*, which were significantly down-regulated in the *Prkci* KD mouse TSCs, are implicated in the regulation of trophoblast differentiation and labyrinth development. Earlier gene KO studies implicated CITED2 in the placental labyrinth formation. However, CITED2 is proposed to have a non-cell-autonomous role in SynT as its function is more important in proper patterning of embryonic capillaries in the labyrinth zone rather than in promoting the SynT differentiation (55). In contrast, KO studies in mouse TSCs indicated that PPAR $\gamma$  is an important regulator for SynT differentiation (32). PPAR $\gamma$ -null mouse TSCs showed specific defects in SynT differentiation and rescue of PPAR $\gamma$  expression rescued *Gcm1* expression and SynT differentiation. Also, earlier, we showed that in mouse TSCs, GATA2 directly regulates expression of several SynT-associated genes including *Gcm1* and, in coordination with GATA3, ensures placental labyrinth development (33). Therefore, we focused our study on GATA2 and PPAR $\gamma$  and further tested their expressions in *Prkci* KD mouse TSCs and PKC $\lambda/1$  KO placenta primordium. We validated the loss of GATA2 and PPAR $\gamma$  protein expressions in *Prkci* KD mouse TSCs (Fig. 5E). Our analyses confirmed that both *Gata2* and *Pparg* mRNA expression are significantly down-regulated in E7.5 PKC $\lambda/1$  KO placenta primordium (Fig. 5F) and the loss of *Gata2* and *Pparg* expression was subsequently associated with impaired transcriptional induction of both *Gcm1* and *Dlx3* in E8.5 PKC $\lambda/1$  KO placentae (Fig. 5G). Thus, our studies in *Prkci* KD mouse TSCs and PKC $\lambda/1$  KO placenta primordium indicated a regulatory pathway, in which the PKC $\lambda/1$  signaling in differentiating TSPCs ensures GATA2 and PPAR $\gamma$  expression, which in turn establishes proper transcriptional program for SynT differentiation (Fig. 5H).

**PKC $\lambda/1$  Is Critical for Human Trophoblast Progenitors to Undergo Differentiation toward SynT Lineage.** Our expression analyses revealed that PKC $\lambda/1$  expression is conserved in CTB progenitors of a first-trimester human placenta. However, functional importance of PKC $\lambda/1$  in the context of human trophoblast development and function has never been tested. We wanted to test whether PKC $\lambda/1$  signaling mediates a conserved function in human CTB progenitors to induce SynT differentiation. However,

testing molecular mechanisms in isolated primary first-trimester CTBs is challenging due to lack of established culture conditions, which could maintain CTBs in a self-renewing stage or could promote their differentiation to SynT lineage. Rather, the recent success of derivation of human TSCs from first-trimester CTBs (34) has opened up opportunities to define molecular mechanisms that control human trophoblast lineage development. When grown in media containing a Wnt activator CHIR99021, EGF, Y27632 (a Rho-associated protein kinase [ROCK] inhibitor), A83-01 and SB431542 (TGF- $\beta$  inhibitors), and valproic acid (a histone deacetylase [HDAC] inhibitor), the established human TSCs can be maintained in a self-renewing stem state for multiple passages. In contrast, when cultured in the presence of cAMP agonist forskolin, human TSCs synchronously differentiate and fuse to form two-dimensional (2D) syncytia on a high-attachment culture plate or 3D cyst-like structures on a low-adhesion culture plate. In both 2D and 3D culture conditions, differentiated human TSCs highly express SynT markers and secrete a large amount of human CG (hCG). Thus, depending on the culture conditions, human TSCs efficiently recapitulate both the self-renewing CTB progenitor state and their differentiation to SynTs. Therefore, we used human TSCs as a model system and performed loss-of-function analyses to test importance of PKC $\lambda/1$  signaling in human TSC self-renewal vs. their differentiation toward the SynT lineage.

We performed lentiviral-mediated shRNA delivery to deplete PKC $\lambda/1$  expression in human TSCs (*PRKCI* KD human TSCs). The shRNA-mediated RNAi in human TSCs reduced *PRKCI* mRNA expression by more than 90% without affecting the *PRKCZ* mRNA expression (Fig. 6A and B), thereby confirming the specificity of the RNAi approach. Similar to *Prkci* KD mouse TSCs, *GATA2*, *PPARG*, and *GCM1* mRNA expressions were significantly reduced in *PRKCI* KD human TSCs (Fig. 6A). Western blot analyses also confirmed loss of GATA2 and PPAR $\gamma$  protein expressions in *PRKCI* KD human TSCs (Fig. 6B). However, the loss of PKC $\lambda/1$  expression in human TSCs did not overtly affect their stem state morphology (Fig. 6C and [SI Appendix, Fig. S5A](#)), proliferation ([SI Appendix, Fig. S5B](#) and [C](#)), or expression of trophoblast stem state markers, such as *TEAD4* or *CDX2* ([SI Appendix, Fig. S5D](#)). Rather, we observed a smaller (~25%) induction in *ELF5* mRNA expression upon loss of PKC $\lambda/1$  ([SI Appendix, Fig. S5D](#)). Thus, we concluded that PKC $\lambda/1$  signaling is not essential to maintain the self-renewing stem state in human TSCs; rather, it is important to maintain optimum expression of key genes like *GATA2*, *PPARG*, and *GCM1*, which are known regulators of SynT differentiation. Therefore, we next interrogated SynT differentiation efficiency in *PRKCI* KD human TSCs.

We cultured control and *PRKCI* KD human TSCs with forskolin on both high- and low-adhesion culture plates to test the efficacy of both 2D and 3D syncytium formation. We assessed 2D SynT differentiation by monitoring elevated mRNA expressions of key SynT-associated genes, such as the HCG $\beta$  components *CGA* and *CGB*; retroviral fusogenic protein *ERVW1*, and pregnancy-associated glycoprotein, *PSG4*. We also tested HCG $\beta$  protein expression and monitored cell syncytialization via loss of E-CADHERIN (CDH1) expression in fused cells. We found strong impairment of SynT differentiation of *PRKCI* KD human TSCs (Fig. 6D–F). Unlike in control human TSCs, mRNA induction of key SynT-associated genes (Fig. 6G) as well as HCG $\beta$  protein expression were strongly inhibited in *PRKCI* KD human TSCs. Furthermore, *PRKCI* KD human TSCs maintained strong expression of CDH1 and showed a near-complete inhibition of cell fusion (Fig. 6E).

The impaired SynT differentiation potential in *PRKCI* KD human TSCs were also evident in the 3D culture conditions. Unlike control human TSCs, which efficiently formed large cyst-like spheres (larger than 50  $\mu$ m in diameter), *PRKCI* KD human TSCs failed to efficiently develop into larger spheres and mainly



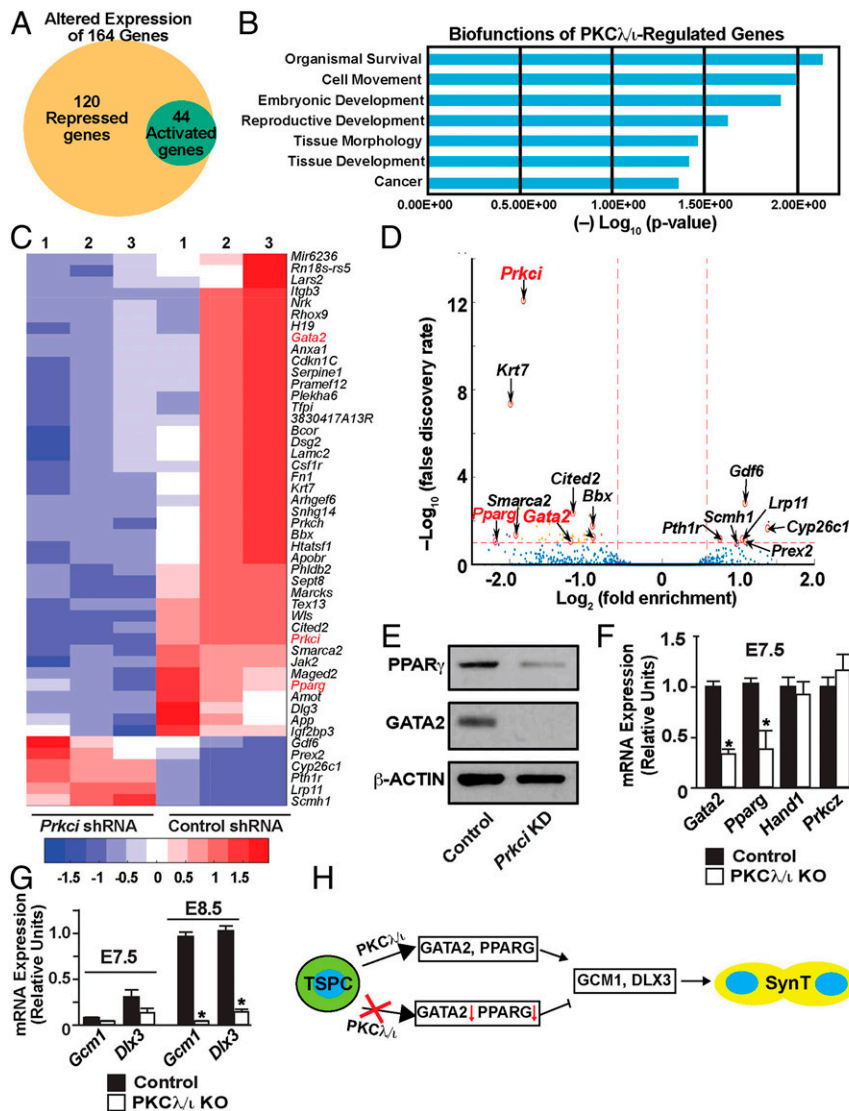


**Fig. 5.** PKC $\lambda/\iota$  signaling regulates expression of GATA2 and PPAR $\gamma$ , key transcription factors for SynT differentiation, in mouse TSCs and primary TSPCs of a mouse placenta primordium. (A) Whole-genome RNA-seq was performed in *Prkci* KD mouse TSCs, and the Venn diagram shows number of genes that were significantly down-regulated (120 genes) and up-regulated (44 genes) upon PKC $\lambda/\iota$  depletion. (B) The plot shows most significant biofunctions (identified via Ingenuity Pathway Analysis) of PKC $\lambda/\iota$ -regulated genes in mouse TSCs. (C and D) Heatmap and volcano plot, respectively, showing significantly altered genes in *Prkci* KD mouse TSCs. Along with *Prkci*, *Gata2* and *Pparg* (marked in red) are among the most significantly down-regulated genes in *Prkci* KD mouse TSCs. (E) Western blot analyses showing loss of GATA2 and PPAR $\gamma$  protein expressions in *Prkci* KD mouse TSCs. (F) Quantitative RT-PCR analyses showing down-regulation of *Gata2* and *Pparg* mRNA expression in TSPCs of E7.5 PKC $\lambda/\iota$  KO placenta primordium (mean  $\pm$  SE;  $n = 4$ ,  $P \leq 0.01$ ). Expression of *Hand1* and *Prkcz* mRNAs remain unaltered. (G) Quantitative RT-PCR analyses in E7.5 and E8.5 PKC $\lambda/\iota$  KO placenta primordia (mean  $\pm$  SE;  $n = 4$ ,  $P \leq 0.001$ ) showing abrogation of *Gcm1* and *Dlx3* induction, which happens between E7.5 and E8.5, in PKC $\lambda/\iota$  KO developing placentae. (H) The model implicates a PKC $\lambda/\iota$ -GATA2/PPAR $\gamma$ -GCM1/DLX3 regulatory axis in SynT differentiation during mouse placentation.

developed smaller cellular aggregates (Fig. 6 H and I). Also, comparative mRNA expression analyses indicated more abundance of *PRKCI* mRNA in a few larger spheres, which were developed with *PRKCI* KD human TSCs, indicating that the large spheres are formed from cells, in which RNAi-mediated gene depletion was inefficient. We noticed significant inhibition of *CGA*, *CGB*, *ERVWI*, and *PSG4* mRNA inductions in the small cell aggregates, which also showed significant down-regulation in *PRKCI* mRNA expressions (Fig. 6J). We also confirmed loss of HCG secretion by *PRKCI* KD human TSCs by measuring HCG concentration in the culture medium (Fig. 6K). Thus, both 2D and 3D SynT differentiation systems revealed impaired SynT differentiation potential of the *PRKCI* KD human TSCs.

**PKC $\lambda/\iota$  Signaling Is Essential for In Vivo SynT Differentiation Potential of Human TSCs.** As discussed above, our in vitro differentiation analysis indicated an important role of PKC $\lambda/\iota$  signaling in inducing SynT differentiation potential in the human TSCs. However, the in vitro differentiation system lacks the complex cellular environment and regulatory factors that control SynT development during placentation. Okae et al. (34) showed that upon subcutaneous (s.c.) injection into nondiabetic-severe combined immunodeficiency mice (NOD-SCID mice), human TSCs invaded the dermal and underlying tissues to establish trophoblastic lesions. These trophoblastic lesions contain cells that represent all cell types of a villous human placenta, namely CTB, SynT, and EVT. Therefore, we next tested in vivo SynT differentiation potential of *PRKCI* KD

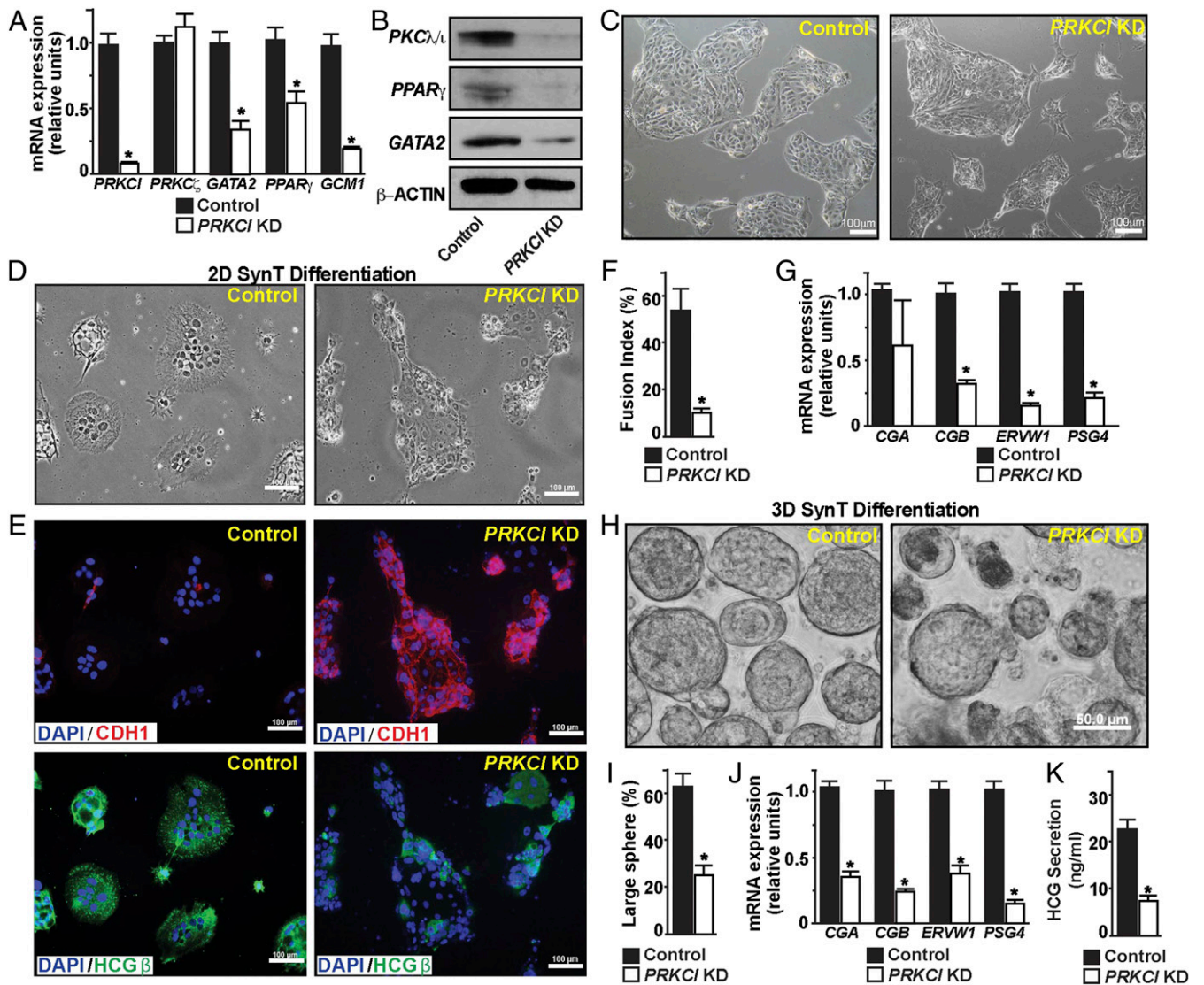


**Fig. 6.** Loss of PKC $\zeta$  impairs SynT differentiation potential in human TSCs. (A) Quantitative RT-PCR analyses showing loss of *GATA2*, *PPARG*, and *GCM1* mRNA expression (mean  $\pm$  SE;  $n = 4$ ,  $P \leq 0.01$ ) upon KD of *PRKCI* in human TSCs (*PRKCI* KD human TSCs). The mRNA expression of *PRKCI* was not affected. (B) Western blots show loss of PKC $\zeta$ , GATA2, and PPAR $\gamma$  protein expressions in *PRKCI* KD human TSCs. (C) Micrographs showing morphology of control and *PRKCI* KD human TSCs. (D and E) Control and *PRKCI* KD human TSCs were subjected to two-dimensional (2D) SynT differentiation on collagen-coated adherent cell culture dishes. Image panels show altered cellular morphology (D); maintenance of E-Cadherin (CDH1) expression (Upper Right in E); and impaired induction of HCG $\beta$  expression (Lower Right in E) in *PRKCI* KD human TSCs. (F) Cell fusion index was quantitated in control and *PRKCI* KD human TSCs. Fusion index was determined by measuring number of fused nuclei with respect to total number of nuclei within image fields (five randomly selected fields from individual experiments were analyzed; three independent experiments were performed). (G) Quantitative RT-PCR analyses showing significant (mean  $\pm$  SE;  $n = 4$ ,  $P \leq 0.001$ ) down-regulation of mRNA expressions of SynT-specific markers in *PRKCI* KD human TSCs, undergoing 2D SynT differentiation. (H) Control and *PRKCI* KD human TSCs were subjected to 3D SynT differentiation on low-attachment dishes. Micrographs show defective SynT differentiation, as assessed from formation of large cell spheres, in *PRKCI* KD human TSCs. (I) Quantification of 3D SynT differentiation efficiency was done by counting large cell spheres (>50  $\mu$ m) from multiple fields (three fields from each experiment; three individual experiments). (J) Quantitative RT-PCR analyses (mean  $\pm$  SE;  $n = 4$ ,  $P \leq 0.001$ ) reveal impaired induction of SynT markers in *PRKCI* KD human TSCs, undergoing 3D SynT differentiation. (K) The plot shows relative levels of HCG, measured by ELISA with culture medium (mean  $\pm$  SE;  $n = 3$ ,  $P \leq 0.001$ ) from control and *PRKCI* KD human TSCs, undergoing SynT differentiation.

human TSCs via transplantation in the NOD-SCID mice (Fig. 7A). Upon transplantation, both control and *PRKCI* KD human TSCs generated tumors with similar efficiency (Fig. 7B), and the presence of human trophoblast cells was confirmed via analyses of human KRT7 expression (Fig. 7C). However, unlike control human TSCs, lesions that were developed from *PRKCI* KD human TSCs were largely devoid of HCG $\beta$ -expressing SynT populations (Fig. 7D). We also confirmed loss of *GATA2* and *GCM1* mRNA expressions in lesions that were developed from *PRKCI* KD human TSCs

(SI Appendix, Fig. S6 A–C). We also tested *PPARG* mRNA levels and found relatively lower expression in lesions generated from *PRKCI* KD human TSCs. However, the reduction level was not statistically significant (SI Appendix, Fig. S6B). Collectively, our in vitro differentiation and in vivo transplantation assays with human TSCs imply an essential and conserved molecular mechanism, in which the PKC $\zeta$  signaling promotes expression of key transcription factors, like GATA2, PPAR $\gamma$ , and GCM1, to assure CTB-to-SynT differentiation.

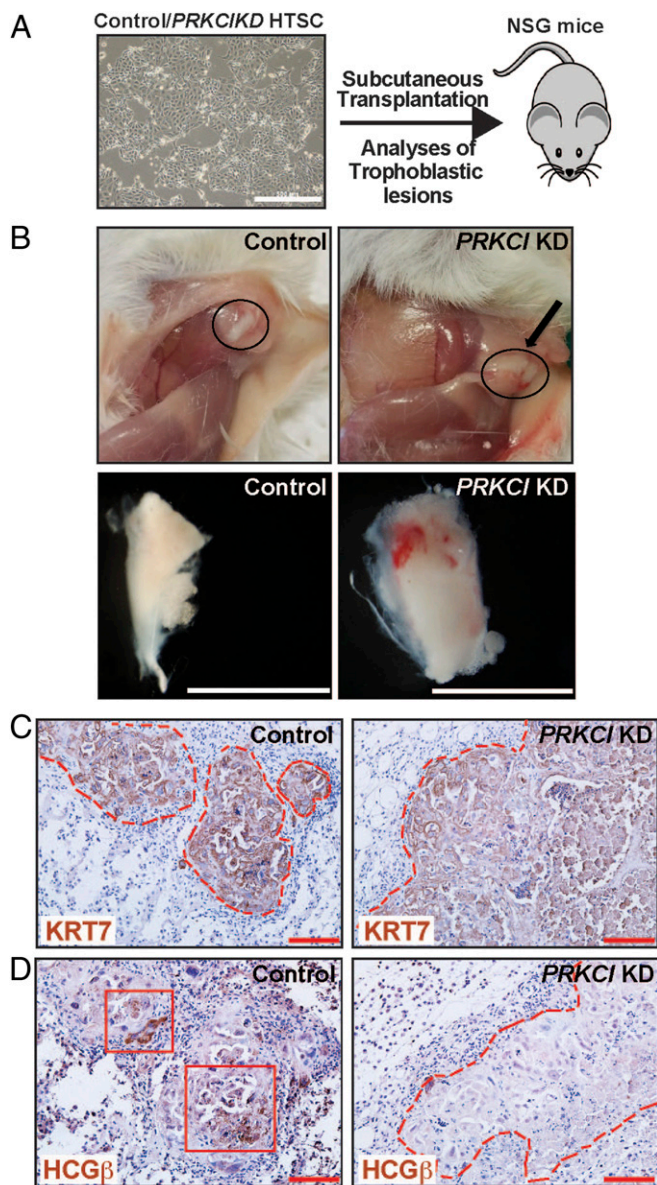


**Fig. 7.** PKC $\lambda/i$  signaling is essential for in vivo SynT differentiation potential of human TSCs. (A) Schematics of testing in vivo developmental potential of human TSC via transplantation assay in NSG mice. Control and PRKCI KD human TSCs were mixed with Matrigel and were s.c. injected into the flank of NSG mice. (B) Images show trophoblastic lesions that were developed from transplanted human TSCs. (Scale bars, 1 cm.) (C and D) Trophoblastic lesions were immunostained with anti-human cyokeratin7 (KRT7) antibody and anti-human HCG $\beta$  antibody, respectively. The trophoblastic lesions that were developed from both control and PRKCI KD human TSCs contained KRT7-expressing human trophoblast cells (C), but the lesions from PRKCI KD human TSCs lacked HCG $\beta$ -expressing trophoblast populations (Right in D), indicating impairment in SynT developmental potential. (Scale bars, 500  $\mu$ m.)

## Discussion

In this study, using both mouse KO models and human TSCs, we have uncovered an evolutionarily conserved function of PKC $\lambda/i$  signaling during trophoblast development and mammalian placentation. In recent years, placental development and the maternal–fetal interaction have been studied with considerable interest as defects in placentation in early postimplantation embryos can lead to either pregnancy failure (1–4), or pregnancy-associated complications like intrauterine growth restriction and preeclampsia

(3–6), or serve as developmental causes for postnatal or adult diseases (7–9). Establishment of the intricate maternal–fetal relationship is instigated by development of the SynT populations, which not only establish the maternal–fetal exchange surface but also modulate the immune function and molecular signaling at the maternal–fetal interface to assure successful pregnancy (56, 57). Our findings in this study indicate that PKC $\lambda/i$ -regulated optimization of gene expression is fundamental to SynT development.

One of the interesting findings of this study is the specific requirement of PKC $\lambda/i$  in establishing the SynT differentiation program. The lack of PKC $\lambda/i$  expression in SynTs within first trimester and term human placentae indicates that PKC $\lambda/i$  signaling is not required for maintenance of SynT function. The specific need of PKC $\lambda/i$  to “prime” trophoblast progenitors for SynT differentiation is further evident from the phenotype of PKC $\lambda/i$ -null mouse embryos. Although PKC $\lambda/i$  is expressed in preimplantation embryos and in TSPCs of placenta primordium, it is not essential for trophoblast cell lineage development at those early stages of embryonic development. Also, the development of TGCs in PKC $\lambda/i$ -null placentae indicates that PKC $\lambda/i$  is dispensable for the development of TGCs, a cell type that is equivalent to human EVT. Rather, PKC $\lambda/i$  is essential for labyrinth development at the onset of chorio-allantoic attachment, indicating a specific need of PKC $\lambda/i$  in nascent SynT population.

Earlier studies with gene KO mice indicated that GCM1 is essential for the placental labyrinth development. The *Gcm1* KO mice die at E10.5 (58) with major defect in SynT development. Our findings in this study show that the PKC $\lambda/i$  signaling is essential to induce both *Gcm1* expression and development of the SynT-II population. We detected presence of a SynA/MCT1-expressing, putative SynT-I trophoblast population in a few PKC $\lambda/i$ -KO placentae. However, development of a matured SynT-I layer was impaired in all PKC $\lambda/i$ -KO placentae.

During mouse placentation, *Dlx3* is initially induced in basal EPC progenitors, which constitutes a layer in chorion and eventually differentiate to SynT-I lineage (17). Later, DLX3 is broadly expressed in both SynT-I and SynT-II population. Defect in SynT development and placental labyrinth formation is also evident in the *Dlx3* KO mice by E9.5 (59). We found that both *Gcm1* and *Dlx3* transcriptions are induced between E7.5 and E8.5, a developmental stage when labyrinth development is initiated upon chorio-allantoic attachment and this induction is impaired in PKC $\lambda/i$ -KO placentae. Not surprisingly, the PKC $\lambda/i$ -KO embryos show a more severe phenotype with complete absence of matured SynTs in the developing placentae.

Our unbiased gene expression analyses in *Prkci* KD mouse TSCs strongly indicate that the PKC $\lambda/i$  signaling ensures TSPC-to-SynT transition by maintaining expression of two conserved transcription factors, GATA2 and PPAR $\gamma$ . Both GATA2 and PPAR $\gamma$  are known regulators of SynT development. We showed that *Gcm1* and *Dlx3* are direct target genes of GATA2 in mouse TSCs (33). Also, loss of PPAR $\gamma$  in mouse TSCs is associated with complete loss of *Gcm1* induction during TSC-to-SynT differentiation (32). Thus, the impairment of *Gcm1* and *Dlx3* induction upon loss of PKC $\lambda/i$  during TSPC-to-SynT transition could be a direct result of the down-regulation of GATA2 and PPAR $\gamma$ .

In this study, we also found that PKC $\lambda/i$ -mediated regulation of GATA2, PPAR $\gamma$ , and GCM1 is a conserved event in the mouse and human TSCs. In a recent study (60), we have shown that GATA2 regulates human SynT differentiation by directly regulating transcription of key SynT-associated genes, such as *CGA*, *CGB*, and *ERVW1*, via formation of a multiprotein complex, including histone demethylase KDM1A and RNA polymerase II, at their gene loci. Based on the conserved nature of GATA2 and PPAR $\gamma$  expression and their regulation by PKC $\lambda/i$  in both mouse and human TSCs, we propose that a conserved PKC $\lambda/i$ -GATA2/PPAR $\gamma$ -GCM1 regulatory axis instigates SynT differentiation during mammalian placentation. We also propose

that the PKC $\lambda$ /i–GATA2/PPAR $\gamma$  signaling axis mediates the progenitor-to-SynT differentiation by modulating global transcriptional program, which also involves epigenetic regulators, like KDM1A. As small molecules could modulate function of most of the members of this regulatory axis, it will be intriguing to test whether or not targeting this regulatory axis could be an option to attenuate SynT differentiation during mammalian placentation.

Another interesting finding of our study is impaired placental and embryonic development upon loss of PKC $\lambda$ /i expression specifically in trophoblast cell lineage. The trophoblast-specific PKC $\lambda$ /i depletion largely recapitulated the placental and embryonic phenotype of the global PKC $\lambda$ /i-KO mice. These results along with selective abundance of the PKC $\lambda$ /i protein expression in TSPCs of postimplantation mouse embryos indicated that the defective embryo patterning in global PKC $\lambda$ /i-KO mice is probably an effect of impaired placentation in those embryos. It is well known that the cells of a gastrulating embryo have signaling cross talks with the TSPCs of a placenta primordium. Furthermore, defect in placentation is a common phenotype in many embryonic lethal mouse mutants. However, we have a poor understanding about how an early defect in labyrinth formation leads to impairment in embryo patterning, and the specific phenotype of PKC $\lambda$ /i-KO mice provides an opportunity to better understand this process. Unfortunately, we do not have access to PKC $\lambda$ /i-conditional KO mouse model, and the lentiviral-mediated shRNA delivery approach did not provide us with an option to deplete PKC $\lambda$ /i in specific trophoblast cell types. During the completion of this study, we are also establishing a mouse model in which we will be able to conditionally delete PKC $\lambda$ /i in specific trophoblast cell types to better understand how PKC $\lambda$ /i functions in nascent SynT lineage and how it regulates the cross talk between the developing embryo proper and the developing placenta. Also, our finding in this study is an implication of PKC $\lambda$ /i signaling in human trophoblast lineage development and function. As defective SynT development could be associated with early pregnancy loss or pregnancy-associated disorders including fetal growth restriction, we also plan to study whether defective PKC $\lambda$ /i function or associated downstream mechanisms are associated with early pregnancy loss and pregnancy-associated disorders.

## Experimental Procedures

**Ethics Statement Regarding Studies with Mouse Model and Human Placental Tissues.** All studies with mouse models were approved by the Institutional Animal Care and Use Committee at the University of Kansas Medical Center (KUMC). Human placental tissues (sixth to ninth weeks of gestation) were obtained from legal pregnancy terminations via the service of Research Centre for Women's and Infants' Health (RCWIH) BioBank at Mount Sinai Hospital, Toronto, Ontario, Canada. The Institutional Review Boards at the KUMC and at the Mount Sinai Hospital approved utilization of human placental tissues and all experimental procedures.

**Collection and Analyses of Mouse Embryos.** Preimplantation embryos were isolated at E2.5 and cultured in KSOM to form matured blastocyst. Ten embryos were used to test for PKC $\lambda$ /i expression via immunostaining. Expressions of PKC $\lambda$ /i in postimplantation mouse embryos (from CD1 and Sv/129 strains) were performed at different developmental stages (E7.5 to E12.5), and representative images of E7.5, E9.5, and E12.5 are shown in this manuscript. At least 10 embryos at each developmental stage were used for the PKC $\lambda$ /i expression studies. The *Prkci* KO mice (B6.129-*Prkci*<sup>tm1Hed</sup>/Mmnc) were obtained from the Mutant Mouse Regional Resource Center, University of North Carolina. The heterozygous animals were bred to obtain litters and harvest embryos at different gestational days. Pregnant female animals were identified by presence of vaginal plug (gestational day 0.5), and embryos were harvested at various gestational days. Uterine horns from pregnant females were dissected out, and individual embryos were analyzed under microscope. Tissues for histological analysis were kept in dry-ice-cooled heptane and stored at –80 °C for cryosectioning. Yolk sacs from each of the dissected embryos were collected, and genomic DNA preparation was done using Extract-N-Amp tissue PCR kit (Sigma; XNAT2). Placenta tissues were collected in RLT buffer, and RNA was extracted using

RNAeasy Mini Kit (Qiagen; 74104). RNA was eluted and concentration was estimated using Nanodrop ND1000 spectrophotometer. For phenotypic analyses of PKC $\lambda$ /i-KO embryos, we analyzed a total of 101 embryos from 11 litters (SI Appendix, Fig. S2A). For phenotypic analyses of *Prkci*-KD embryos, we analyzed 35 control embryos and 36 *Prkci*-KD embryos from eight individual experiments (SI Appendix, Fig. S4A).

**Collection and Analyses of Human Placentae.** First-trimester placentae were obtained via services from RCWIH Biobank, Toronto. Normal-term placentae ( $\geq 38$  wk of gestation) were collected from cesarean delivery at the KUMC. For PKC $\lambda$ /i expression analyses, eight first-trimester placentae (sixth to ninth weeks of gestation) were sectioned and immunostained. Additionally, six normal-term placentae were used for expression analyses.

**Human TSC Culture.** Human TSC lines, derived from first-trimester CTBs, were described earlier (34). Although multiple lines were used, the data presented in this manuscript were generated using CT27 human TSC line. Human TSCs were cultured in DMEM/F12 supplemented with Heparin and L-glutamine along with mixture of inhibitors. We followed the established protocol by T.A.'s group and induced SynT differentiation using forskolin. Both male and female human TSC lines were used for initial experimentation. To generate *PRKCI* KD human TSCs, shRNA-mediated RNAi was performed. For initial screening, both male and female cell lines were used. As we did not notice any phenotypic difference after *PRKCI* depletion, a female *PRKCI* KD human TSC line and corresponding control set were used for subsequent experimentation.

**Trophoblast-Specific *Prkci* KD.** Morula from day 2.5 plugged CD-1 super-ovulated females were treated with acidic Tyrode's solution for removal of zona pellucida. The embryos were immediately transferred to EmbryoMax Advanced KSOM media. Embryos were treated with viral particles having either control pLKO.3G empty vector or shRNA against *Prkci* for 5 h. The embryos were washed two to three times, subsequently incubated overnight in EmbryoMax Advanced KSOM media, and transferred into day 0.5 pseudopregnant females the following day. Uterine horns of control and KD sets were harvested at day 9.5. Placental tissue was obtained for RNA preparation to validate KD efficiency. Embryos were either dissected or kept frozen for sectioning purpose.

**Transplantation of Human TSCs into NSG Mice.** For transplantation analyses in NSG mice, control and *PRKCI* KD human TSCs were mixed with Matrigel and used to inject s.c. into the flank of NSG mice (6–9 wk old). A total of  $10^7$  cells was used for each transplantation experiment. Mice were killed after 7 d, and trophoblastic lesions generated were isolated, photographed, measured for size, fixed, embedded in paraffin, and sectioned for further analyses. Three individual experiments were performed, and six mice (three for control human TSCs and three for *PRKCI*-KD human TSCs) were used in each experiment.

**Statistical Significance.** Statistical significances were determined for quantitative RT-PCR analyses, analyses of SynT-differentiation efficiency and HCG secretion by human TSCs. We have performed at least  $n = 3$  experimental replicates for all of those experiments. For statistical significance of generated data, statistical comparisons between two means were determined with Student's *t* test. Although in a few figures studies from multiple groups are presented, the statistical significance was tested by comparing data of two groups, and significantly altered values ( $P \leq 0.05$ ) are highlighted in figures by an asterisk. RNA-seq data were generated with  $n = 3$  experimental replicates per group. The statistical significance of altered gene expression (twofold change) was initially confirmed with right-tailed Fisher's exact test with *P* value cutoff set at 0.01. The final list of altered genes that were presented in Fig. 5C was selected with an additional FDR cutoff set at 0.1. The raw data for RNA-seq analyses have been deposited and are available in the GEO database (accession no. GSE100285).

Additional details of experimental procedures are mentioned in SI Appendix.

**ACKNOWLEDGMENTS.** This research was supported by NIH Grants HD062546, HD101319, HD0098880, and HD079363; bridging grant support under the Kansas Idea Network of Biomedical Research Excellence (P20GM103418) to S.P.; a University of Kansas Biomedical Research Training Program grant to B.B.; and a NIH Center of Biomedical Research Program (P30GM122731) pilot grant to P.H. This study was supported by various core facilities, including the Genomics Core, Transgenic and Gene Targeting Institutional Facility, Imaging and Histology Core Facility, and the Bioinformatics Core of the University of Kansas Medical Center.

1. K. Cockburn, J. Rossant, Making the blastocyst: Lessons from the mouse. *J. Clin. Invest.* **120**, 995–1003 (2010).
2. R. M. Roberts, S. J. Fisher, Trophoblast stem cells. *Biol. Reprod.* **84**, 412–421 (2011).
3. J. Rossant, J. C. Cross, Placental development: Lessons from mouse mutants. *Nat. Rev. Genet.* **2**, 538–548 (2001).
4. P. L. Pfeffer, D. J. Pearson, Trophoblast development. *Reproduction* **143**, 231–246 (2012).
5. C. W. Redman, I. L. Sargent, Latest advances in understanding preeclampsia. *Science* **308**, 1592–1594 (2005).
6. L. Myatt, Placental adaptive responses and fetal programming. *J. Physiol.* **572**, 25–30 (2006).
7. P. D. Gluckman, M. A. Hanson, C. Cooper, K. L. Thornburg, Effect of in utero and early-life conditions on adult health and disease. *N. Engl. J. Med.* **359**, 61–73 (2008).
8. K. M. Godfrey, D. J. Barker, Fetal nutrition and adult disease. *Am. J. Clin. Nutr.* **71** (suppl. 5), 1344S–1352S (2000).
9. E. F. Funai *et al.*, Long-term mortality after preeclampsia. *Epidemiology* **16**, 206–215 (2005).
10. A. M. Carter, Animal models of human placentation—a review. *Placenta* **28**, 541–547 (2007).
11. J. Rossant, Stem cells from the mammalian blastocyst. *Stem Cells* **19**, 477–482 (2001).
12. D. G. Simmons, A. L. Fortier, J. C. Cross, Diverse subtypes and developmental origins of trophoblast giant cells in the mouse placenta. *Dev. Biol.* **304**, 567–578 (2007).
13. D. G. Simmons, J. C. Cross, Determinants of trophoblast lineage and cell subtype specification in the mouse placenta. *Dev. Biol.* **284**, 12–24 (2005).
14. P. Kaufmann, S. Black, B. Huppertz, Endovascular trophoblast invasion: Implications for the pathogenesis of intrauterine growth retardation and preeclampsia. *Biol. Reprod.* **69**, 1–7 (2003).
15. G. X. Rosario, T. Konno, M. J. Soares, Maternal hypoxia activates endovascular trophoblast cell invasion. *Dev. Biol.* **314**, 362–375 (2008).
16. M. J. Soares *et al.*, Regulatory pathways controlling the endovascular invasive trophoblast cell lineage. *J. Reprod. Dev.* **58**, 283–287 (2012).
17. D. G. Simmons *et al.*, Early patterning of the chorion leads to the trilaminar trophoblast cell structure in the placental labyrinth. *Development* **135**, 2083–2091 (2008).
18. E. Basyuk *et al.*, Murine *Gcm1* gene is expressed in a subset of placental trophoblast cells. *Dev. Dyn.* **214**, 303–311 (1999).
19. M. Knofler *et al.*, Human placenta and trophoblast development: Key molecular mechanisms and model systems. *Cell. Mol. Life Sci.* **76**, 3479–3496 (2019).
20. J. L. James, A. M. Carter, L. W. Chamley, Human placentation from nidation to 5 weeks of gestation. Part I: What do we know about formative placental development following implantation? *Placenta* **33**, 327–334 (2012).
21. A. L. Boss, L. W. Chamley, J. L. James, Placental formation in early pregnancy: How is the centre of the placenta made? *Hum. Reprod. Update* **24**, 750–760 (2018).
22. S. Haider *et al.*, Notch1 controls development of the extravillous trophoblast lineage in the human placenta. *Proc. Natl. Acad. Sci. U.S.A.* **113**, E7710–E7719 (2016).
23. A. E. Beer, J. O. Sio, Placenta as an immunological barrier. *Biol. Reprod.* **26**, 15–27 (1982).
24. M. Yang, Z. M. Lei, C. Rao, The central role of human chorionic gonadotropin in the formation of human placental syncytium. *Endocrinology* **144**, 1108–1120 (2003).
25. M. A. Costa, The endocrine function of human placenta: An overview. *Reprod. Biomed. Online* **32**, 14–43 (2016).
26. L. A. Cole, hCG, the wonder of today's science. *Reprod. Biol. Endocrinol.* **10**, 24 (2012).
27. M. PrabhuDas *et al.*, Immune mechanisms at the maternal–fetal interface: Perspectives and challenges. *Nat. Immunol.* **16**, 328–334 (2015).
28. L. W. Chamley *et al.*, Review: Where is the maternofetal interface? *Placenta* **35**, S74–S80 (2014).
29. J. Rossant, Lineage development and polar asymmetries in the peri-implantation mouse blastocyst. *Semin. Cell Dev. Biol.* **15**, 573–581 (2004).
30. B. Stecca *et al.*, *Gcm1* expression defines three stages of chorio-allantoic interaction during placental development. *Mech. Dev.* **115**, 27–34 (2002).
31. L. Anson-Cartwright *et al.*, The glial cells missing-1 protein is essential for branching morphogenesis in the chorioallantoic placenta. *Nat. Genet.* **25**, 311–314 (2000).
32. M. M. Parast *et al.*, PPARgamma regulates trophoblast proliferation and promotes labyrinthine trilineage differentiation. *PLoS One* **4**, e8055 (2009).
33. P. Home *et al.*, Genetic redundancy of GATA factors in the extraembryonic trophoblast lineage ensures the progression of preimplantation and postimplantation mammalian development. *Development* **144**, 876–888 (2017).
34. H. Okae *et al.*, Derivation of human trophoblast stem cells. *Cell Stem Cell* **22**, 50–63.e6 (2018).
35. M. Zhu, C. Y. Leung, M. N. Shahbazi, M. Zernicka-Goetz, Actomyosin polarisation through PLC-PKC triggers symmetry breaking of the mouse embryo. *Nat. Commun.* **8**, 921 (2017).
36. D. Dutta *et al.*, Self-renewal versus lineage commitment of embryonic stem cells: Protein kinase C signaling shifts the balance. *Stem Cells* **29**, 618–628 (2011).
37. G. Rajendran *et al.*, Inhibition of protein kinase C signaling maintains rat embryonic stem cell pluripotency. *J. Biol. Chem.* **288**, 24351–24362 (2013).
38. B. Mahato *et al.*, Regulation of mitochondrial function and cellular energy metabolism by protein kinase C- $\lambda$ : A novel mode of balancing pluripotency. *Stem Cells* **32**, 2880–2892 (2014).
39. M. Leitges *et al.*, Targeted disruption of the zetaPKC gene results in the impairment of the NF-kappaB pathway. *Mol. Cell* **8**, 771–780 (2001).
40. R. S. Soloff, C. Katayama, M. Y. Lin, J. R. Feramisco, S. M. Hedrick, Targeted deletion of protein kinase C lambda reveals a distribution of functions between the two atypical protein kinase C isoforms. *J. Immunol.* **173**, 3250–3260 (2004).
41. S. Seidl *et al.*, Phenotypical analysis of atypical PKCs in vivo function display a compensatory system at mouse embryonic day 7.5. *PLoS One* **8**, e62756 (2013).
42. N. Saiz, J. B. Grabarek, N. Sabherwal, N. Papalopulu, B. Plusa, Atypical protein kinase C couples cell sorting with primitive endoderm maturation in the mouse blastocyst. *Development* **140**, 4311–4322 (2013).
43. A. Dupressoir *et al.*, Syncytin-A knockout mice demonstrate the critical role in placental of a fusogenic, endogenous retrovirus-derived, envelope gene. *Proc. Natl. Acad. Sci. U.S.A.* **106**, 12127–12132 (2009).
44. A. Nagai, K. Takebe, J. Nio-Kobayashi, H. Takahashi-Iwanaga, T. Iwanaga, Cellular expression of the monocarboxylate transporter (MCT) family in the placenta of mice. *Placenta* **31**, 126–133 (2010).
45. D. S. Lee, M. A. Rumi, T. Konno, M. J. Soares, In vivo genetic manipulation of the rat trophoblast cell lineage using lentiviral vector delivery. *Genesis* **47**, 433–439 (2009).
46. P. Home *et al.*, Altered subcellular localization of transcription factor TEAD4 regulates first mammalian cell lineage commitment. *Proc. Natl. Acad. Sci. U.S.A.* **109**, 7362–7367 (2012).
47. D. Strumpf *et al.*, *Cdx2* is required for correct cell fate specification and differentiation of trophoblast in the mouse blastocyst. *Development* **132**, 2093–2102 (2005).
48. A. P. Russ *et al.*, Eomesodermin is required for mouse trophoblast development and mesoderm formation. *Nature* **404**, 95–99 (2000).
49. P. A. Latos *et al.*, Fgf and Esrrb integrate epigenetic and transcriptional networks that regulate self-renewal of trophoblast stem cells. *Nat. Commun.* **6**, 7776 (2015).
50. M. Donnison *et al.*, Loss of the extraembryonic ectoderm in *Elf5* mutants leads to defects in embryonic patterning. *Development* **132**, 2299–2308 (2005).
51. V. Nadeau *et al.*, *Map2k1* and *Map2k2* genes contribute to the normal development of syncytiotrophoblasts during placental development. *Development* **136**, 1363–1374 (2009).
52. B. Lichtner, P. Knaus, H. Lehrach, J. Adjaye, BMP10 as a potent inducer of trophoblast differentiation in human embryonic and induced pluripotent stem cells. *Biomaterials* **34**, 9789–9802 (2013).
53. B. Mikic, K. Rossmeier, L. Bierwert, Identification of a tendon phenotype in *GDF6* deficient mice. *Anat. Rec. (Hoboken)* **292**, 396–400 (2009).
54. D. E. Clendenning, D. P. Mortlock, The BMP ligand *Gdf6* prevents differentiation of coronal suture mesenchyme in early cranial development. *PLoS One* **7**, e36789 (2012).
55. S. L. Withington *et al.*, Loss of *Cited2* affects trophoblast formation and vascularization of the mouse placenta. *Dev. Biol.* **294**, 67–82 (2006).
56. J. D. Aplin *et al.*, IFPA Meeting 2016 Workshop Report III: Decidua-trophoblast interactions; trophoblast implantation and invasion; immunology at the maternal–fetal interface; placental inflammation. *Placenta* **60** (suppl. 1), S15–S19 (2017).
57. M. Pavličev *et al.*, Single-cell transcriptomics of the human placenta: Inferring the cell communication network of the maternal–fetal interface. *Genome Res.* **27**, 349–361 (2017).
58. J. Schreiber *et al.*, Placental failure in mice lacking the mammalian homolog of glial cells missing, *GCMa*. *Mol. Cell. Biol.* **20**, 2466–2474 (2000).
59. M. I. Morasso, A. Grinberg, G. Robinson, T. D. Sargent, K. A. Mahon, Placental failure in mice lacking the homeobox gene *Dlx3*. *Proc. Natl. Acad. Sci. U.S.A.* **96**, 162–167 (1999).
60. J. Milano-Foster *et al.*, Regulation of human trophoblast syncytialization by histone demethylase *LSD1*. *J. Biol. Chem.* **294**, 17301–17313 (2019).